Published in final edited form as:
FEBS Lett. 2010 March 19; 584(6): 1133–1138. doi:10.1016/j.febslet.2010.02.015.

Design and characterization of a constitutively open KcsA

Luis G. Cuello[1], **Vishwanath Jogini**[1], **D. Marien Cortes**[1], **Amornrat Somporpisut**[1], **Michael D. Purdy**[3], **Michael C. Wiener**[3], and **Eduardo Perozo**[1,2]

[1]Department of Biochemistry and Molecular Biology. The University of Chicago. 929 E 57th Street, Chicago, IL 60637 USA.

[2]Institute for Biophysical Dynamics. The University of Chicago. 929 E 57th Street, Chicago, IL 60637 USA.

[3]Department of Molecular Physiology and Biological Physics, University of Virginia Charlottesville, VA, 22906 USA.

Abstract

The molecular nature of the structure responsible for proton sensitivity in KcsA has been identified as a charge cluster that surrounds the inner helical bundle gate. Here, we show that this proton sensor can be modified to engineer a constitutively open form of KcsA, amenable to functional, spectroscopic and structural analyses. By combining charge neutralizations for all acidic and basic residues in the cluster at positions 25, 117–122 and 124 (but not E118), a mutant KcsA is generated that displays constitutively open-channel activity up to pH 9. The structure of this mutant revealed that full opening appears to be inhibited by lattice forces since the activation gate seems to be only on the early stages of opening.

1. INTRODUCTION

Most Potassium channels switch from a non-conductive to a conductive conformation by structural rearrangements in two regions of the permeation path, the inner helical bundle, located at the intracellular end of the channel [1–8] and the selectivity filter, towards the extracellular face of the channel [9–17]. In potassium channels, the inner helical bundle moves during activation/deactivation gating, initiating stimulus-dependent ion conduction [3,4,6–8, 18–21].

Activation gating requires an energy transduction step where a specialized region of the channel converts specific types of physical stimuli (i.e. voltage, ligand binding, force, etc.) into protein motion. This is the case, for example, of the voltage sensing domain in voltage dependent channels [22,23] or the ligand binding domain in cys-loop receptors [24,25]. The nature of this transduction step in the prokaryotic K^+ channel KcsA has recently been elucidated. A cluster of charged residues located at the intracellular end of TM1 and TM2 was identified as the proton sensor [26,27]. This charge cluster exerts attractive/repulsive forces that stabilize the inner bundle helices in its closed or open conformations in a proton-dependent way.

Correspondence to: Eduardo Perozo, eperozo@uchicago.edu, Ph: (773) 243-6580, Fax: (773) 834-4632.

Here, we have pursued strategies to engineer a constitutively open channel by modifying the electrostatic balance within the pH sensor charge cluster. The basic approach relies on combining mutants, both in TM1 and TM2 segments, to bias the closed-open equilibrium towards the open conformation. We show that a charge-less KcsA mutant background with the additional mutations H25Q and the presence of E118 as a charged group have an additive effect when combined on the same open reading frame, generating channels that appear to be constitutively open at neutral pH. This also suggest that the interaction between these two charges is only partial.

2. METHODS

Side directed mutagenesis, protein expression and purification

Wild-type and the H25Q/E118+ mutant were expressed and purified as described previously [28], with some modifications. Briefly, fresh competent XL10 cells were transformed with WT KcsA-pQE32. Solubilization was carried out with 10 mM DDM in PBS with 1mM PMSF, at pH 7.5, for 1 hour at RT. spun down at 100,000 g for 1 hour and purified with Co^{2+} resin. The channel was eluted with 50 mM Tris and 150mM KCl containing 5mM DM.

Functional assays

Complementation growth assays were performed as described [26] by transforming LB2003 cells with a plasmid containing the test construct. Cell growth was evaluated in liquid or solid define media with 1 mM KCl and supplemented with 0.5 mM IPTG. Macroscopic $^{86}Rb^{+}$ uptake experiments follow our described protocols for KcsA [29] using 10 mM citrate-phosphate buffer and a Dowex 50-X8 column to remove extra-vesicular $^{86}Rb^{+}$. Liposome patch clamp experiments follow the protocols laid out in [14], with the channels reconstituted into asolectin vesicles at a 1:10,000 protein to lipid ratio (mass:mass).

EPR spectroscopy

Standard X-band CW EPR spectra were obtained from spin labeled and reconstituted channels as previously decribed [4] using a Bruker ELEXYS spectrometer equipped with a super High-Q resonator at 2 mW incident power, 100 kHz modulation frequency and 1 G modulation amplitude.

Electrostatic calculations

Electrostatic potential grid maps were calculated using the linearized Poisson Boltzmann equation by the Adaptive Poisson-Boltzmann Solver (APBS) plug-in [30] within VMD [31], as described in detail in [26] these calculations assume bulk pKa values for the ionizable side chains. Electrostatic potential maps were displayed using Pymol (http://pymol.sourceforge.net).

Crystallization of constitutively open KcsA

KcsA open mutant was expressed and purified to homogeneity. Protein stability was assessed by SDS protein-gels, western blot and gel filtration. The KcsA open mutant was crystallized in the presence of antibody Fab fragment by sitting drop method as described previously [32]. Cubic shaped crystal of KcsA-Fab complex appeared after a week in a sitting drop with the following composition 20–25 % PEG400 (v/v), 50 mM magnesium acetate, 50 mM sodium acetate (pH 5.4–5.6) at 20 °C. Crystals diffracted to Bragg spacing of 2.5 Å. Data was collected on beamline 22ID (SER-CAT) at the Advanced Photon Source and processed with HKL2000 [33]. Since the expected structure is in the open state, we used only Fab fragment and extracellular part of WT KcsA (PDB 1K4C) without the selectivity filter as search model for solving the structure by molecular replacement. In the first cycle of refinement using CNS

[34]electron density corresponding to the intracellular part showed up, which is filled up with the transmembrane helices by manual rebuilding using O[35]. Multiple cycles of manual rebuilding and refinement was carried out till the complete model is built into the electron density and the Rfactors are lowered. Data collection and refinement statistics are given in Table 1.

3. RESULTS

Engineering a constitutively open KcsA

All of the available experimental data [26,27,36] points to the fundamental role played by the cluster of charged residues surrounding the inner bundle gate in determining KcsA proton-dependent activation gating. Based on this, and the evidence supporting to the role of electrostatic repulsion as the basis for gate opening in KcsA [26], we reasoned that the best strategy to engineer a constitutively open channel was to modify the electrostatic balance of the charge cluster to bias the closed-open equilibrium towards the open conformation. Initially, we focused on a charge-less construct where all members of the cluster in the pH sensor have been mutated to Glutamines (Fig 1A).

The presence of a glutamic acid at position 118 in a charge-less background (mutant E118+) promotes a sharp right-shift in the pH-dependence of the activation curve[26]. Another potential candidate for charge engineering is E118 putative electrostatic partner, residue H25 (Fig 1B). When neutralized by substitution to glutamine, H25Q also induces a large shift in the pH dependence of activation, leading to an increased level of channel activity at neutral pH (by $^{86}Rb^{+}$ flux assays)[26]. If the H25-E118 interaction is exclusive (i.e. forming an ion pair), the double mutant H25Q/E118+ should not have an additive effect when combined on the same open reading frame. Alternatively, a through-space Coulombic interaction would maximize inter-helix repulsion and stabilize the inner bundle gate in it open conformation at neutral pH. This is shown qualitatively by solving the Poisson-Boltzmann equation [30] using the H25Q/E118+ mutant and calculating the electrostatic surface potential at the KcsA inner helical bundle. Figure 1C shows slices through the calculated isopotential contours at ± 1kT/e (~25 mV) in 150 mM KCl pH 7, for a truncated form (without C-terminal or N-terminal helices) of wt-KcsA (Fig. 1C, top) and the H25Q/E118+ mutant (Fig. 1C, bottom), as a projected through the core of the inner gate/pH sensor (inset). wt-KcsA is characterized by alternating positive and negative fields which, we have proposed, stabilize the inner helical bundle in its closed conformation [26]. In contrast, the mutant H25Q/E118+ is characterized by an excess negative potential field generated by the sole negative charge at E118. This would result in constitutively open channel.

Conformation of the activation gate

The properties of this open KcsA mutant (H25Q-E118+) were evaluated by four independent approaches. When used to transform the strain LB 2003 strain, which is incapable of growing in low potassium media without an active K^{+}-selective transporter [37], H25Q-E118+ channels were able to strongly complement LB 2003 growth in both liquid culture (Figure 2A) or agar plates (not shown), compared with wt-KcsA or the positive substitution H25R. Also, reconstituted H25Q-E118+ channels showed a large shift in the apparent pKa of activation (pKa=7.9 ± 0.1) to more basic pH as judged from $^{86}Rb^{+}$ uptake experiments, so that a large fraction of the total $^{86}Rb^{+}$ influx is already evident at neutral pH (Figure 2B).

These macroscopic estimations of channel activity suggested that the H25Q-E118+ mutant show a higher level of activity under conditions where wild-type KcsA is functionally silent. To investigate the precise functional correlate of this constitutively open gate channel we carried out stationary liposome patch clam measurements. In sharp contrast with WT-KcsA,

electrophysiological recordings of H25Q-E118+ at basic pH (8.0) show robust, single channel activity, which persists at steady state (Fig. 3). Under these conditions the single channel activity of H25Q-E118+ gradually decreases with time, as C-type inactivation sets in (not shown). Change to an intracellular acidic pH has only subtle effect, as steady state NPo decrease about 20 % (Fig 3B-C). This apparent reduction in open probability could be explained by titration of the remaining charge (E118), thus reducing the electrostatic repulsion among TM2 helices.

Finally, we evaluated the extent of gate opening in H25Q-E118+ channels by EPR spectroscopy, monitoring the extent of spin-spin dipolar coupling with a spin label at position G116. Fig. 3 shows that in WT-KcsA spectral broadening is gradually reduced in a pH-dependent way, since lowering pH promotes gate opening, increasing the inter-spin distance and reducing the degree of dipolar coupling [4]. In contrast, the constitutively open channel shows no significant pH-dependent conformational changes in a wide pH range and the extent of the dipolar broadening is compatible with a fully open inner bundle gate. These results clearly establish that the inner bundle gate in the H25Q-E118+ mutant is permanently open at neutral pH and that this opening is at least equivalent to that of WT-KcsA at low pH.

Towards the structure of open KcsA

The constitutively open H25Q/E118+ represents an excellent target to further understand the structural basis of activation gating in KcsA. This construct was crystallized using a similar approach as that used to obtain the high resolution structure of closed KcsA [32]. To this end, a Fab antibody (generously provided by R. MacKinnon) was used to make a channel-Fab complex, which crystallized in the I4 space group [32]. The structure of H25Q/E118+ was solved to 2.5 Å resolution using molecular replacement methods. Unexpectedly, under present conditions the structure of H25Q/E118+ represents a conformation of KcsA unexpectedly similar to its closed structure (1K4C), although it revealed a slight opening at the bundle crossing (Figure 4). We found that the distance difference between C_α of the closed and the partial open state at residue T111 is 3 Å within the subunit and the extent of opening is ~ 4 Å at the C_α level.

Even though the present structure of H25Q/E118+ is fairly similar in conformation to the closed state, the small structural changes observed throughout TM1 and TM2 can be used to address basic questions regarding the opening mechanism in KcsA. The Cα-Cα RMSD between the closed structure (1K4C) and H25Q/E118+, illustrates that the core of the channel remains essentially unchanged, but their differences increase sharply beyond two apparent hinge points, G30 in TM1 and G104 in TM2 (Fig. 5B). This is in contrast to the expected hinge point at G99, based on the structure of fully open MthK [19]. When the relative variation of the B-factors around the local mean for specific regions of the protein are mapped onto the H25Q/E118+ structure (Fig. 5C), it is clear that the local disorder also increases sharply beyond the two hinge points described above. Although comparing absolute B-factors for structures of different resolutions is not straightforward, contrasting B-factor deviations (variance) [14] allows for a more meaningful comparison of local (versus lattice) disorder. High B-factor variance at the intracellular end of TM1 and TM2 suggests that unbalancing of the charge cluster by means of the H25Q/E118+ mutant, makes the helix bundle highly unstable resulting in channel opening, but that local disorder is enhanced by contrary lattice forces, which ultimately prevent the gate from fully opening.

4. DISCUSSION

Development of a constitutively open KcsA provides a unique opportunity to advance the study of the molecular basis of gating in a system amenable to a wide variety of functional, spectroscopic and structural approaches. Indeed, Thompsom *et al* [27] have identified a set of

mutations that render KcsA constitutively open at neutral pH, but in contrast to our open KcsA mutant (H25Q/E118+), their strategy was focused on developing a residual positive electrostatic field, based on the triple mutant H25R/E118A/E120A. Thus, whether there is a local positive or negative field at the end of the inner bundle gate, helix-helix electrostatic repulsion seems to be the driving force for activation gating in KcsA.

A mutant trapped in the open conformation at neutral pH will finally allow cysteine reactivity experiments like the substituted-cysteine accessibility method (SCAM) [38] to be performed in KcsA. Further, such a mutant will be essential to tease out detailed interactions between the activation and inactivation gates, from a functional and structural dynamics perspective. But more importantly, the present mutant construct will serve as a key target to attempt direct structural studies of the open conformation of this channel. This we have vigorously pursued using an Fab-channel complex as previously shown for the closed channel [32]. Unexpectedly, the channel was only partially open and the overall structure was nearer the closed state than the expected open state (Figure 4). However, a more careful analysis of this structure revealed that the diagonally-related subunit C_α distance difference at residue 111 between the closed and the partial open state is 3 Å. Structural comparison of the two conformations point that at least at this degree of opening, the gating hinge in KcsA is located not at G99, as is typically expected from comparisons with open MthK [19], but it shifts almost two turns of a helix at residue G104. This finding, if confirmed at larger degrees of opening, suggest a wider range of hinge locations than previously thought. The large B-factors observed at the intracellular side of KcsA TM1 and TM2 are clear indicators of local disorder, suggesting that by disrupting the channel electrostatic gate (the gatekeeper), the inner helical bundle becomes unstable. At the same time, it is likely that the present set of crystal contacts inhibits the more complete gate opening suggested by our functional measurements. Close inspection of the protein-Fab crystal lattice reveals that the crystal packing is likely opposing the expanding lateral forces exerted by electrostatic repulsion in our KcsA-open mutant and thus, the present construct is not conducive to the determination of the structure of full open KcsA. An ongoing effort, based on lattice engineering, has allowed for the determination of KcsA in its fully open and a host of partially open conformations.

Acknowledgments

We thank Drs. B. Roux H Mchaourab and R. Nakamoto for helpful discussions and comments on the manuscript. S. Chakrapani, J. Cordero-Morales, O. Dalmas, J Santos and the members of the Perozo lab for experimental advice and comments on the manuscript. Assistance and support by Jim Fait and the staff at SER-CAT, at the Advanced Photon Source, is greatly appreciated. This work was supported in part by NIH grant R01-GM57846 and by a gift from the Palmer family.

REFERENCES

1. Doyle DA, Morais Cabral J, Pfuetzner RA, Kuo A, Gulbis JM, Cohen SL, Chait BT, MacKinnon R. The structure of the potassium channel: molecular basis of K+ conduction and selectivity. Science 1998;280:69–77. [PubMed: 9525859]
2. Holmgren M, Shin KS, Yellen G. The activation gate of a voltage-gated K+ channel can be trapped in the open state by an intersubunit metal bridge. Neuron 1998;21:617–621. [PubMed: 9768847]
3. Liu Y, Holmgren M, Jurman ME, Yellen G. Gated access to the pore of a voltage-dependent K+ channel. Neuron 1997;19:175–184. [PubMed: 9247273]
4. Perozo E, Cortes DM, Cuello LG. Three-dimensional architecture and gating mechanism of a K+ channel studied by EPR spectroscopy. Nat Struct Biol 1998;5:459–469. [PubMed: 9628484]
5. Perozo E, Cortes DM, Cuello LG. Structural rearrangements underlying K+- channel activation gating. Science 1999;285:73–78. [PubMed: 10390363]
6. Webster SM, Del Camino D, Dekker JP, Yellen G. Intracellular gate opening in Shaker K+ channels defined by high-affinity metal bridges. Nature 2004;428:864–868. [PubMed: 15103379]

7. Yellen G. The moving parts of voltage-gated ion channels. Quarterly Reviews of Biophysics 1998;31:239–295. [PubMed: 10384687]
8. del Camino D, Holmgren M, Liu Y, Yellen G. Blocker protection in the pore of a voltage-gated K+ channel and its structural implications. Nature 2000;403:321–325. [PubMed: 10659852]
9. Liu Y, Jurman ME, Yellen G. Dynamic rearrangement of the outer mouth of a K+ channel during gating. Neuron 1996;16:859–867. [PubMed: 8608004]
10. Chapman ML, VanDongen HM, VanDongen AM. Activation-dependent subconductance levels in the drk1 K channel suggest a subunit basis for ion permeation and gating. Biophys J 1997;72:708–719. [PubMed: 9017198]
11. Chapman ML, VanDongen AM. K channel subconductance levels result from heteromeric pore conformations. J Gen Physiol 2005;126:87–103. [PubMed: 16043772]
12. Gao L, Mi X, Paajanen V, Wang K, Fan Z. Activation-coupled inactivation in the bacterial potassium channel KcsA. Proc Natl Acad Sci U S A 2005;102:17630–17635. [PubMed: 16301524]
13. Blunck R, Cordero-Morales JF, Cuello LG, Perozo E, Bezanilla F. Detection of the opening of the bundle crossing in KcsA with fluorescence lifetime spectroscopy reveals the existence of two gates for ion conduction. J Gen Physiol 2006;128:569–581. [PubMed: 17043150]
14. Cordero-Morales JF, Cuello LG, Zhao Y, Jogini V, Cortes DM, Roux B, Perozo E. Molecular determinants of gating at the potassium-channel selectivity filter. Nat Struct Mol Biol 2006;13:311–318. [PubMed: 16532009]
15. Chakrapani S, Cordero-Morales JF, Perozo E. A quantitative description of KcsA gating II: single-channel currents. J Gen Physiol 2007;130:479–496. [PubMed: 17938231]
16. Chakrapani S, Cordero-Morales JF, Perozo E. A quantitative description of KcsA gating I: macroscopic currents. J Gen Physiol 2007;130:465–478. [PubMed: 17938230]
17. Cordero-Morales JF, Jogini V, Lewis A, Vasquez V, Cortes DM, Roux B, Perozo E. Molecular driving forces determining potassium channel slow inactivation. Nat Struct Mol Biol 2007;14:1062–1069. [PubMed: 17922012]
18. Liu YS, Sompornpisut P, Perozo E. Structure of the KcsA channel intracellular gate in the open state. Nat Struct Biol 2001;8:883–887. [PubMed: 11573095]
19. Jiang Y, Lee A, Chen J, Cadene M, Chait BT, MacKinnon R. The open pore conformation of potassium channels. Nature 2002;417:523–526. [PubMed: 12037560]
20. Jiang Y, Lee A, Chen J, Cadene M, Chait BT, MacKinnon R. Crystal structure and mechanism of a calcium-gated potassium channel. Nature 2002;417:515–522. [PubMed: 12037559]
21. Kelly BL, Gross A. Potassium channel gating observed with site-directed mass tagging. Nat Struct Biol 2003;10:280–284. [PubMed: 12640442]
22. Bezanilla F. How membrane proteins sense voltage. Nat Rev Mol Cell Biol 2008;9:323–332. [PubMed: 18354422]
23. Swartz KJ. Sensing voltage across lipid membranes. Nature 2008;456:891–897. [PubMed: 19092925]
24. Changeux JP, Edelstein SJ. Allosteric mechanisms of signal transduction. Science 2005;308:1424–1428. [PubMed: 15933191]
25. Sine SM, Engel AG. Recent advances in Cys-loop receptor structure and function. Nature 2006;440:448–455. [PubMed: 16554804]
26. Cuello L, Jogini V, Cortes DM, Somporpisut A, Perozo E. A molecular mechanism for proton-dependent gating in KcsA. 2009 Accompanying manuscript.
27. Thompson AN, Posson DJ, Parsa PV, Nimigean CM. Molecular mechanism of pH sensing in KcsA potassium channels. Proc Natl Acad Sci U S A 2008;105:6900–6905. [PubMed: 18443286]
28. Cortes DM, Perozo E. Structural dynamics of the Streptomyces lividans K+ channel (SKC1): oligomeric stoichiometry and stability. Biochemistry 1997;36:10343–10352. [PubMed: 9254634]
29. Cuello LG, Romero JG, Cortes DM, Perozo E. pH-dependent gating in the Streptomyces lividans K + channel. Biochemistry 1998;37:3229–3236. [PubMed: 9536962]
30. Baker NA, Sept D, Joseph S, Holst MJ, McCammon JA. Electrostatics of nanosystems: application to microtubules and the ribosome. Proc Natl Acad Sci U S A 2001;98:10037–10041. [PubMed: 11517324]

31. Humphrey W, Dalke A, Schulten K. VMD: visual molecular dynamics. J Mol Graph 1996;14:33–38. 27–28. [PubMed: 8744570]

32. Zhou Y, Morais-Cabral JH, Kaufman A, MacKinnon R. Chemistry of ion coordination and hydration revealed by a K+ channel-Fab complex at 2.0 A resolution. Nature 2001;414:43–48. [PubMed: 11689936]

33. Otwinowski Z, M W. Processing of X-ray diffraction data collected in oscillation mode. Methods in Enzymology 1997;276:307–332.

34. Brunger AT, et al. Crystallography & NMR system: A new software suite for macromolecular structure determination. Acta Crystallogr D Biol Crystallogr 1998;54:905–921. [PubMed: 9757107]

35. Jones TA, Zou JY, Cowan SW, Kjeldgaard M. Improved methods for building protein models in electron density maps and the location of errors in these models. Acta Crystallogr A 1991;47(Pt 2): 110–119. [PubMed: 2025413]

36. Paynter JJ, Sarkies P, Andres-Enguix I, Tucker SJ. Genetic selection of activatory mutations in KcsA. Channels (Austin) 2008;2:413–418. [PubMed: 18797191]

37. Stumpe S, Bakker EP. Requirement of a large K+-uptake capacity and of extracytoplasmic protease activity for protamine resistance of Escherichia coli. Arch Microbiol 1997;167:126–136.

38. Akabas MH, Stauffer DA, Xu M, Karlin A. Acetylcholine receptor channel structure probed in cysteine-substitution mutants. Science 1992;258:307–310. [PubMed: 1384130]

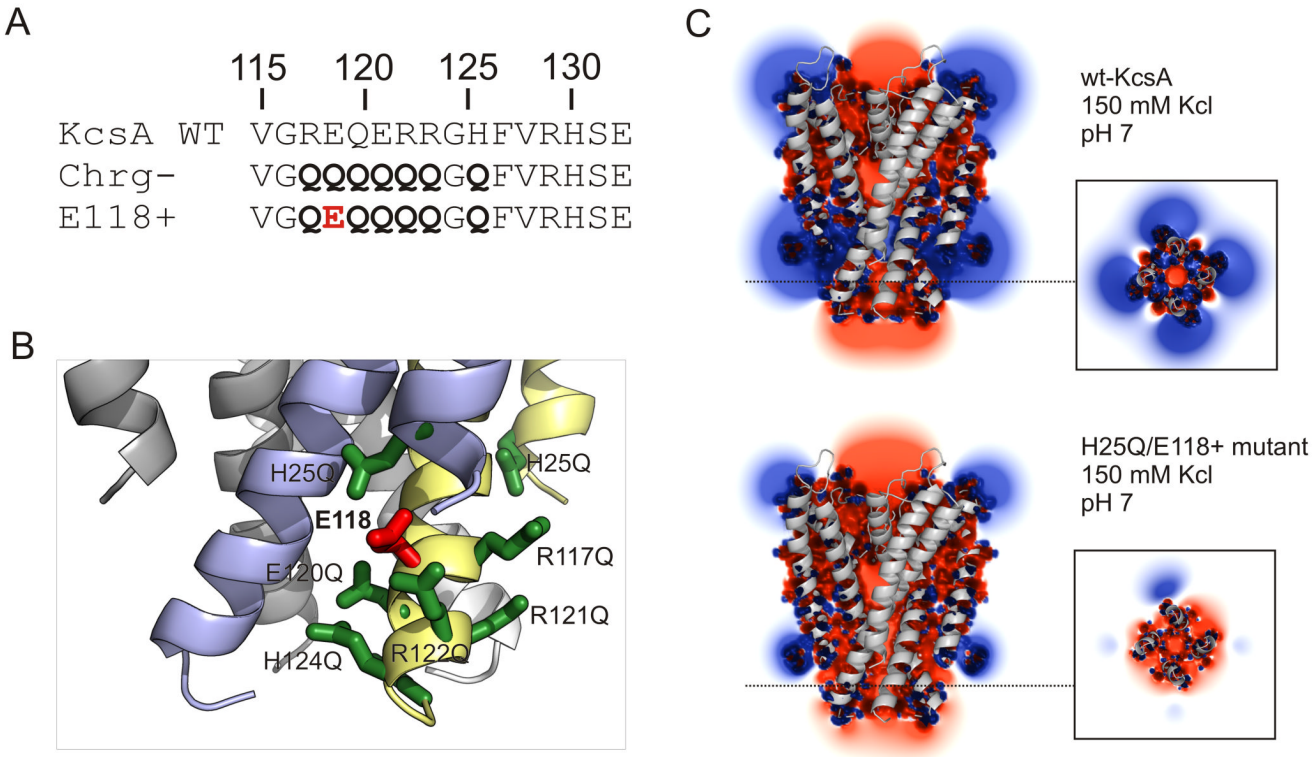

Figure 1. Designing a constitutively open KcsA by electrostatic repulsion

A. Mutational strategy to generate a pH sensor with an individual ionizable side chain. Key charges in TM1 and TM2 were neutralized to glutamine (charge-less background) and this served as background to reintroduce the individual residues one-by one. Mutations represented by bold letters. **B**. Ribbon representation of the intracellular bundle region of the mutant H25Q-E118+, highlighting the cluster of charges responsible for pH-dependent activation. Neutralized residues are shown in green, residue E118 in red. This constitutively open mutant was created by combining systematically neutralization of residues H25 at the TM1 and R117, E120, R121, R122 and H124 at the TM2. **C**. Isopotential surface at the KcsA inner helical bundle calculated from the solution to the Poisson-Boltzmann equation [30]. Shown are slices through the center of the channel and across the pH sensor charge cluster (inset) for wt-KcsA at pH 7 (top) and the H25Q/E118+ mutant in 150 mM KCl. Calculated isopotential contours at 1kT/e (~25mV).

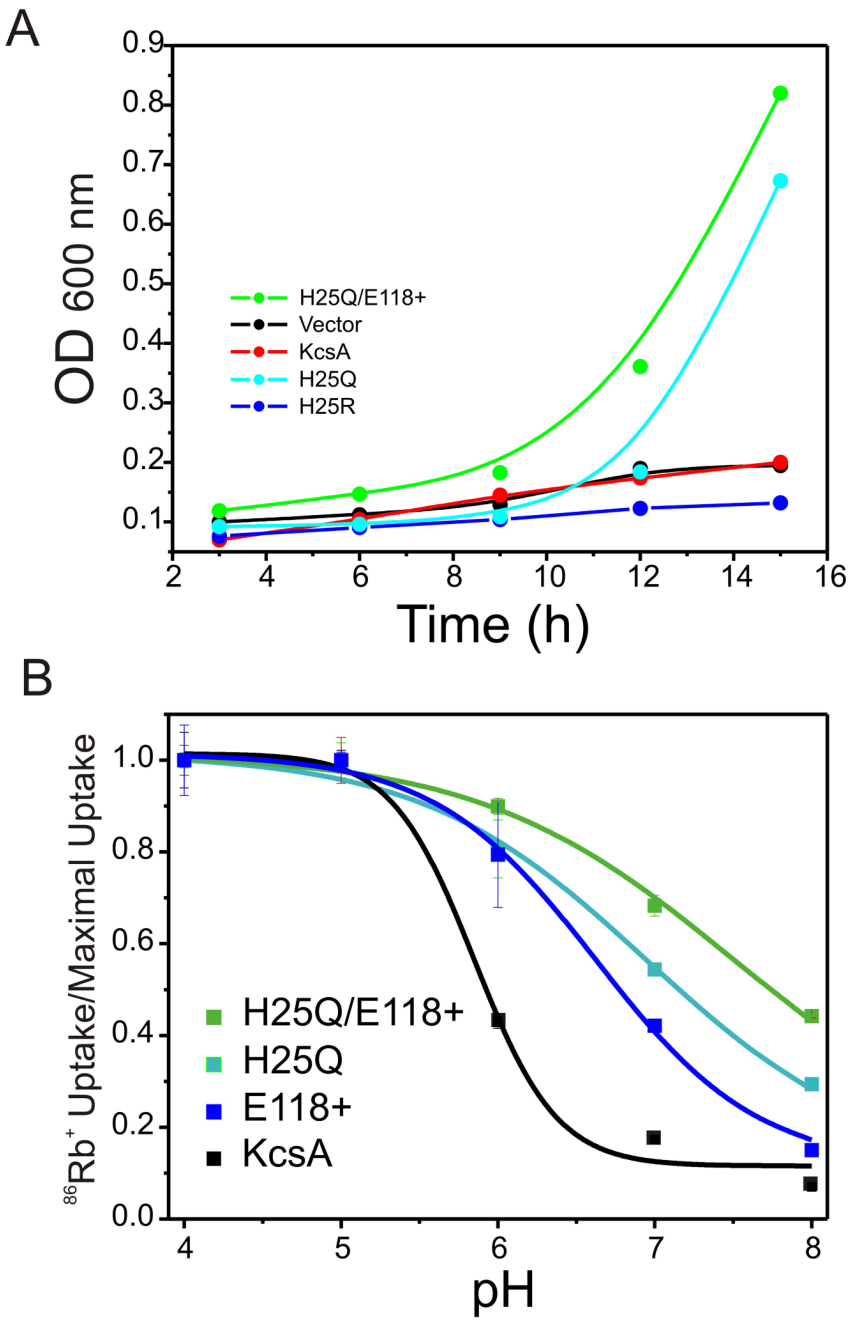

Figure 2. Macroscopic functional assays

A. LB 2003 *E. coli* strain complementation assay of KcsA mutants. KcsA mutants H25Q and H25Q-E118+ are capable of complement growth of the bacteria in a low potassium concentration media (1 mM KCl). KcsA-wt, H25R mutant and an empty expression vector fail to recovery the cells in the same growing conditions. **B**. ^{86}Rb uptake experiments of constitutively KcsA open mutants H25Q, E118+ and the combination H25Q-E118+. Activation pKa: KcsA-wt=5.89±0.2, H25Q=7.09±0.48, E118+6.78 and the combination H25Q-E118+=7.68±0.2

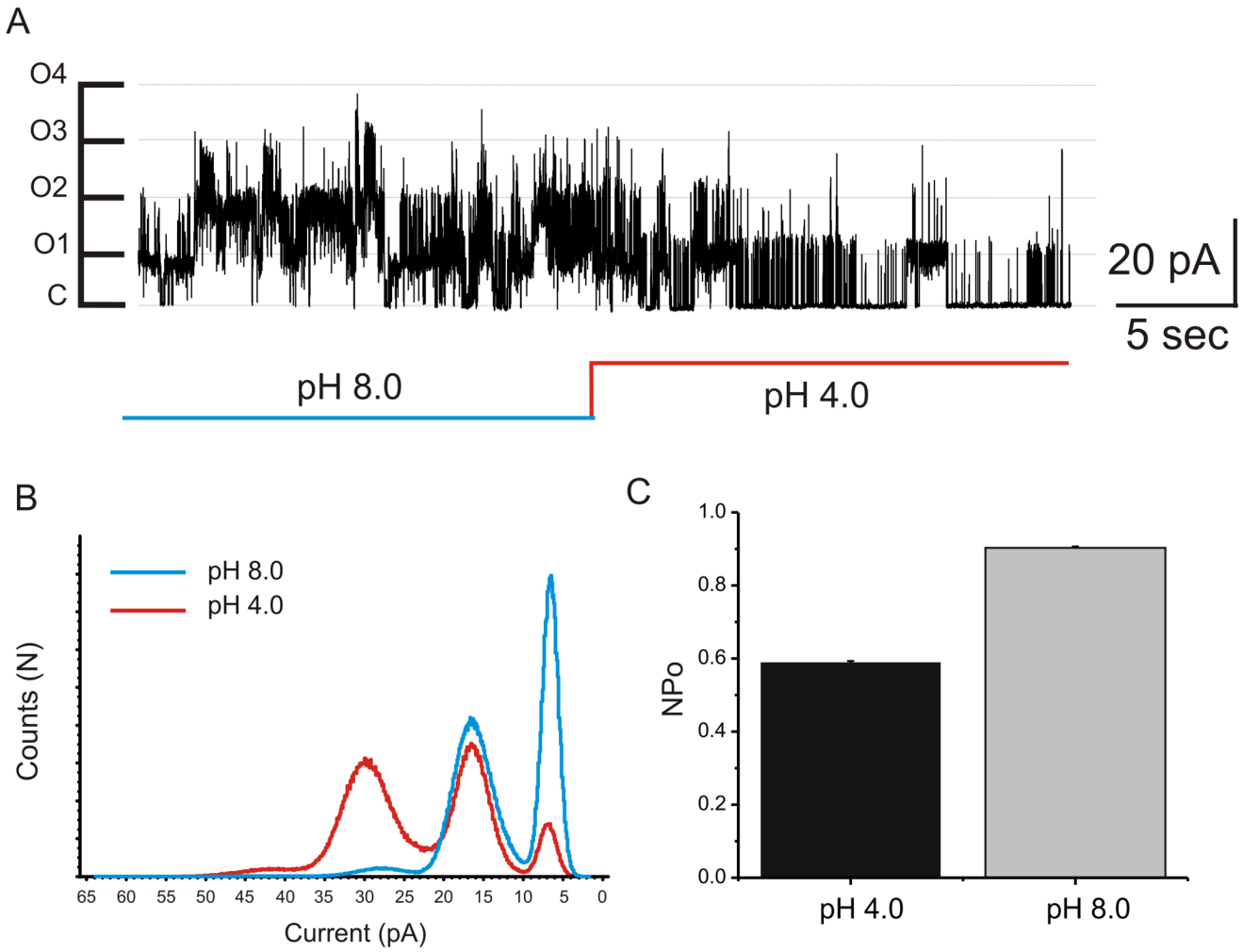

Figure 3. Single channel properties of H25Q/E118+

A. Single channel activity of H25Q-E118+ at different pH values. Overall activity in this multi-channel patch decreases slightly by changing from pH 8.0 to 4.0. Single channel currents were evoked at +100 mV in symmetric 200 mM KCl solution. **B**. All points histogram of the record in A. **C**. Estimated stationary NPo values for H25Q-E118+ at two pH values. Data shown as mean ± sd, for an n=4.

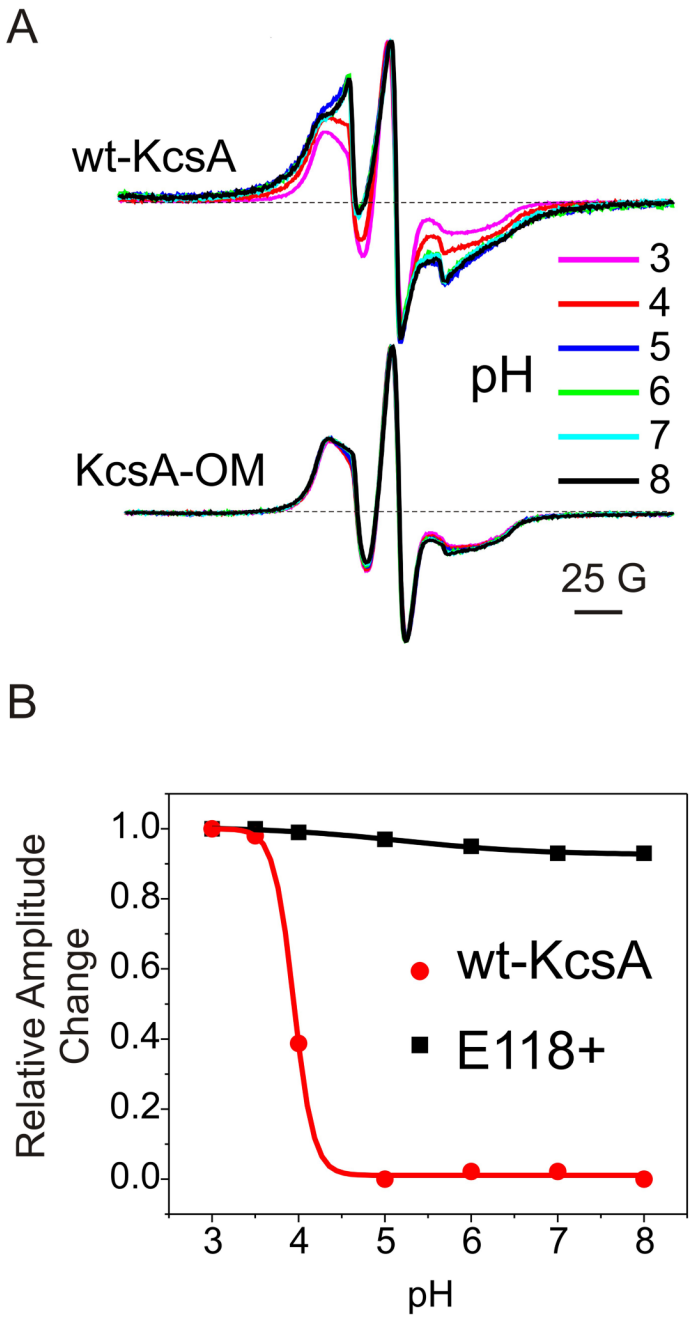

Figure 4. Conformation of the inner bundle gate

EPR spectra of the KcsA-G116C-SL (top) and H25Q-E118+-G116C-SL (bottom) depicting changes in dipolar spin-spin coupling at different pH values. The right panel shows the dependence of the relative extent of opening at the lower gate on pH for KcsA-G116C-SL (red) and H25Q-E118+-G116C-SL (black). For the open-mutant, the dipolar coupling is similar to that of KcsA at pH 3.0 for all pH values.

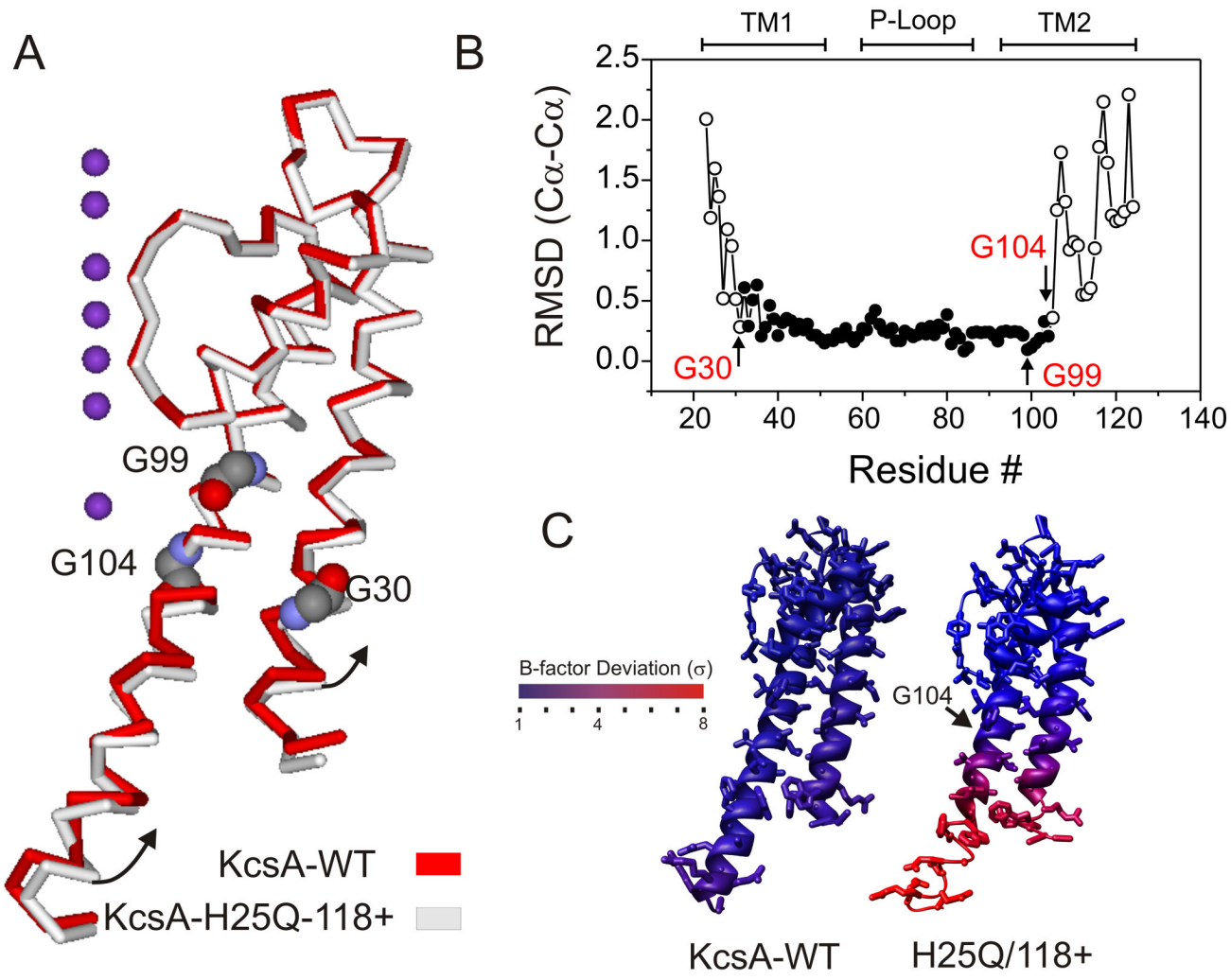

Figure 5. X-ray structure of H25Q/E118+

A. Structural alignment of wt-KcsA (1K4C=red ribbons) and KcsAH25Q-E118+ open mutant (white ribbons). Potassium ions (blue) and key residues (G99 in MthK and G104 in KcsA open-mutant) for TM2 hinge movement (gray) are represented as sphere. Black arrows indicate the direction of TM2 movement. **B**. Comparison of Cα-Cα RMSD between the closed structure (1K4C) and H25Q/E118+. In red are highlighted pivot points along the TM segment presumably important for the gating process. Major changes are seen before residue G30 and after residue G104 (open circles), while the core of the protein remain unchanged (filled circles). In the H25Q-E118+-KcsA mutant, the hinge point seems to be around G104 in contrast with the position G99 predicted based in MthK structure. **C.** Mapping of B-factors variation on top of wt-KcsA (1K4C) according a color code scale. High B-factor variances are clearly seen at the intracellular end of TM1 and TM2.

Table 1

Data collection and refinement statistics

	KcsA H25Q-E118+
Data collection	
Space group	I4
Cell dimensions	
a, b, c (Å)	156.62, 156.62, 75.3
α, β, γ (°)	90.0, 90.0, 90.0
Resolution (Å)	50.0-2.5
R_{merge} or R_{sym} (%)[a,b]	5.0 (26.9)
$I/\sigma I$	33.5 (4.5)
Completeness (%)[a]	99.5 (97.8)
Redundancy	4.4 (4.1)
Refinement	
Resolution (Å)	50.0-2.5
No. reflections	31,067
R_{work} / R_{free} (%)[c]	22.9/25.9
No. atoms	
Protein	3,922
Ion	7
Lipid	41
Water	12
B-factors	
Protein	55.94
Ion	35.70
Water	50.33
R.m.s deviations	
Bond lengths (Å)[d]	0.006
Bond angles (°)[d]	1.349

[a] Values in parentheses are for the highest-resolution shell (2.15 Å – 2.05 Å).

[b] $R_{symm} = \Sigma | I - \langle I \rangle | / \Sigma \langle I \rangle$

[c] $R = \Sigma| Fo - Fc| / \Sigma Fo$, 10% of the data that were excluded in the refinement were used in the R_{free} calculation.

[d] RMSD of bond is the root-mean-square deviation of bond angle and length.